View metadata, citation and similar papers at core.ac.uk

brought to you by CORE

provided by ePrints@Bangalore University

Transp Porous Med (2017) 120:605–631
DOI 10.1007/s11242-017-0943-8

Linear and Weakly Nonlinear Stability Analyses of Two-Dimensional, Steady Brinkman–Bénard Convection Using Local Thermal Non-equilibrium Model

P. G. Siddheshwar[1] · **C. Siddabasappa**[1]

Received: 19 May 2017 / Accepted: 21 September 2017 / Published online: 9 October 2017
© Springer Science+Business Media B.V. 2017

Abstract Effect of local thermal non-equilibrium (LTNE) on onset of Brinkman–Bénard convection and on heat transport is investigated. Rigid–rigid and free–free, isothermal boundaries are considered for investigation. The assumption of LTNE leads to an 'advanced onset' situation compared to that predicted by the local thermal equilibrium (LTE) assumption. This results in the 'enhanced heat transport' situation in the problem. Asymptotic analysis for small and large values of inter-phase heat transfer coefficient is also carried out on critical Rayleigh number, critical wave number and Nusselt number. In respect of boundary influences on onset and heat transport, it is found that classical results hold even under the LTNE assumption. The other parameters' influences on onset and heat transport are qualitatively similar in LTNE and LTE cases.

Keywords Brinkman–Bénard convection · Porous media · Rigid–rigid · Free–free · Monodisperse · LTNE · Nonlinear

List of symbols

Latin symbols

A, B, C	Amplitudes of linear regime (m)
c_p	Specific heat at constant pressure (Jkg^{-1}K^{-1})
d	Channel depth (m)
D, E	Amplitudes of nonlinear regime (m)
$\mathbf{g}$	Acceleration due to gravity (ms^{-2})
h	Inter-phase heat transfer coefficient (Wm^{-2}K^{-1})

✉ P. G. Siddheshwar
mathdrpgs@gmail.com

1 Department of Mathematics, Jnana Bharathi Campus, Bangalore University, Bangalore 560056, India

H	Dimensionless inter-phase heat transfer coefficient
k	Wave number in the x direction (m^{-1})
K	Permeability (m^2)
P	Pressure ($kgm^{-1}s^{-2}$)
Pr	Prandtl number
$\mathbf{q}$	Filtration velocity or Darcy velocity (ms^{-1})
Ra	Thermal Rayleigh number
t	Time (s)
T	Temperature (K)
u	Horizontal velocity component (ms^{-1})
w	Vertical velocity component (ms^{-1})
x, z	Cartesian coordinate
X, Z	Dimensionless coordinates

Greek symbols

α	Thermal expansion coefficient (K^{-1})
γ	Porosity-modified ratio of thermal conductivities
Γ	Ratio of thermal diffusivities
Λ	Viscosity ratio
κ	Thermal conductivity ($Wm^{-1}K^{-1}$)
μ	Dynamic viscosity ($kgm^{-1}s^{-1}$)
μ'	Effective dynamic viscosity ($kgm^{-1}s^{-1}$)
ϕ	Porosity ($0 < \phi < 1$)
Ψ	Dimensionless stream function
ρ	Density (kgm^{-3})
σ^2	Inverse Darcy number or porous parameter
τ	Dimensionless time
Θ	Dimensionless temperature

Subscripts or superscripts

0	Reference value
b	Basic state
c	Critical
FF	Free–free
l	Liquid
LTE	Local thermal equilibrium
LTNE	Local thermal non-equilibrium
RR	Rigid–rigid
s	Solid

1 Introduction

Liquids have generally been the most commonly used medium of transporting heat away from high-temperature regions. In other words, liquids have been serving as cooling agents. With the need to store energy came the application of the concept of a liquid-saturated porous medium. The weak thermal conductivity of the material making up the porous medium in comparison with the thermal conductivity of the liquid ensured that the residence time of heat was more. Most earlier studies on free convection of liquids in a porous medium were based on the assumption that there is local thermal equilibrium (LTE) between the occupying liquid and the porous medium. Subsequently, it was realized that it might be wrong to assume equilibrium, and hence, there appeared in the literature works connected with free convection of liquids in a porous medium with local thermal non-equilibrium (LTNE) between the two phases. Typically in a thermal convection problem, the solid phase becomes hot fast and retains heat for a shorter time compared to the liquid phase and hence acts as a heat source in the medium and the liquid turns out to be a heat sink of same strength as the source but obviously with opposite sign.

Rayleigh–Bénard convection of liquids in a porous medium is by now a well-investigated problem using either LTE or LTNE assumptions (Lapwood 1948; Straus 1974; Banu and Rees 2002; Nield et al. 2002; Postelnicu and Rees 2003; Rudraiah et al. 2003; Malashetty et al. 2005a, b; Nield and Bejan 2006; Straughan 2006, 2010, 2015; Postelnicu 2008; Bhadauria and Agarwal 2011; Lee et al. 2011; Saravanan and Sivakumar 2011; Shivakumara et al. 2011a, b; Barletta and Rees 2012; Nield 2012; Celli et al. 2013, 2017; Dehghan et al. 2014; Nield and Kuznetsov 2014; Barletta et al. 2015; Kaviany 2012;Vafai 2015; Lagziri et al. 2016; Nield et al. 2016 and references therein). The thermal problems with LTNE effects are little more involved than the ones with LTE effect. What makes the former problem more interesting and challenging is that the heat transport equations of liquid and solid phases have features of both parabolic and hyperbolic equations (Rees et al. 2008). Further, a biharmonic term arises in these equations in addition to the harmonic term. Browsing the literature pertaining to LTNE effects on Rayleigh–Bénard convection in liquids occupying porous medium, it becomes amply clear that the following aspects have been considered in the reported problems:

(i) Linear and weakly nonlinear/energy stability of the problem have been studied in both low-porosity and high-porosity media (Banu and Rees 2002; Postelnicu and Rees 2003; Rees and Pop 2005; Malashetty et al. 2005a, b;Malashetty et al. 2005a; Straughan 2006, 2010, 2015; Postelnicu 2008; Lee et al. 2011; Saravanan and Sivakumar 2011; Shivakumara et al. 2011a, b; Barletta and Rees 2012; Celli et al. 2013). Siddheshwar et al. (2017) showed that minimal modes are good enough to study linear and nonlinear stability of Brinkman–Bénard convection in a porous medium with LTNE assumptions. Sunil and Mahajan (2011) considered the effect of rotation and made an energy stability analysis of the problem.

(ii) Except for the work of Postelnicu (2008) on Brinkman–Bénard convection, most of the works on this problem consider the rather unrealistic stress-free boundary condition.

The objective of this paper is to consider the following unconsidered aspects of the Brinkman–Bénard convection problem (Rayleigh–Bénard convection in a high-porosity medium):

(a) Asymptotic small H and large H analyses of critical wave number and Rayleigh number in the case of rigid–rigid, isothermal boundary. Similar study in free–free boundaries was reported by Postelnicu and Rees (2003).

(b) Asymptotic analysis of Nusselt number in the case of rigid–rigid and free–free, isothermal boundaries.

(c) LTNE as a ‘heat transport enhancing mechanism.’

2 Mathematical Formulation

The governing equations for studying steady two-dimensional Brinkman–Bénard convection (see Fig. 1) in the case when there is local thermal non-equilibrium between liquid and solid phases are:

$$\nabla.\mathbf{q} = 0, \tag{1}$$

$$\frac{\rho}{\phi}\frac{\partial \mathbf{q}}{\partial t} = -\nabla P + \mu_l^{'}\nabla^2\mathbf{q} - \frac{\mu_l}{K}\mathbf{q} + \rho_l\mathbf{g}, \tag{2}$$

$$(\rho c_p)_l\left(\phi\frac{\partial T_l}{\partial t} + (\mathbf{q}.\nabla)T_l\right) = \phi\kappa_l\nabla^2 T_l + h(T_s - T_l), \tag{3}$$

$$(1-\phi)(\rho c_p)_s\frac{\partial T_s}{\partial t} = (1-\phi)\kappa_s\nabla^2 T_s - h(T_s - T_l), \tag{4}$$

$$\rho(T) = \rho(T_0)(1 - \alpha(T_l - T_0)). \tag{5}$$

The inertial term is neglected in Eq. (2) since we are considering only small-scale convective motions. Non-dimensionalizing Eqs. (1)–(4) using

$$\left.\begin{array}{l} (X, Z) = \left(\dfrac{x}{d}, \dfrac{z}{d}\right), \quad \mathbf{q^*} = \left(\dfrac{(\rho c_p)_l d}{\phi\kappa_l}\right)\mathbf{q}, \quad \Theta_l = \dfrac{T_l}{\Delta T}, \\ \Theta_s = \dfrac{T_s}{\Delta T}, \quad \tau = \left(\dfrac{\kappa_l}{(\rho c_p)_l d^2}\right)t, \quad P^* = \left(\dfrac{d^2(\rho c_p)_l}{\phi\mu_l\kappa_l}\right)P, \end{array}\right\}, \tag{6}$$

the dimensionless form of governing equations is

$$\nabla.\mathbf{q^*} = 0, \tag{7}$$

$$\frac{1}{Pr}\frac{\partial}{\partial\tau}\mathbf{q^*} = -\nabla^* P^* + \Lambda\nabla^{*2}\mathbf{q^*} - \sigma^2\mathbf{q^*} + [R_1 - Ra_l(\Theta_l - \Theta_0)], \tag{8}$$

$$\frac{\partial\Theta_l}{\partial\tau} = \nabla^{*2}\Theta_l + H(\Theta_s - \Theta_l) - (\mathbf{q^*}.\nabla^*)\Theta_l, \tag{9}$$

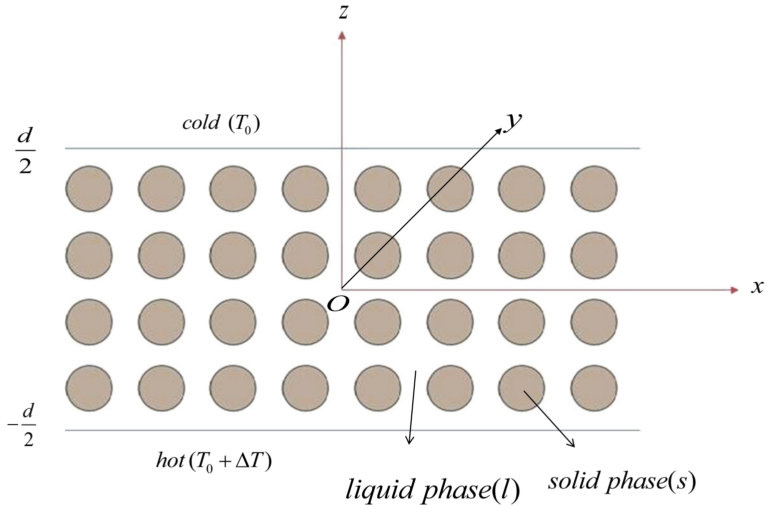

Fig. 1 Schematic of the physical configuration

$$\Gamma \frac{\partial \Theta_s}{\partial \tau} = \nabla^{*2}\Theta_s - \gamma H(\Theta_s - \Theta_l), \tag{10}$$

where

$$\begin{aligned}
Pr &= \frac{\mu_l (\rho c_p)_l}{\phi \rho_l \kappa_l},\\
Ra_l &= \frac{\rho_l (\rho c_p)_l \alpha g d^3 \Delta T}{\phi \kappa_l \mu_l}, \quad R_1 = \frac{Ra_l}{\alpha \Delta T},\\
\Lambda &= \frac{\mu_l'}{\mu_l}, \quad \sigma^2 = \frac{d^2}{K},\\
H &= \frac{h d^2}{\phi \kappa_l}, \quad \gamma = \frac{\phi \kappa_l}{(1-\phi)\kappa_s},\\
\Gamma &= \frac{\kappa_l (\rho c_p)_s}{\kappa_s (\rho c_p)_l}.
\end{aligned}$$

At this point, we note that

$$Ra_l = \sigma^2 Ra_D, \tag{11}$$

where Ra_D is the Darcy–Rayleigh number. We continue our analysis with Ra_l only since sparsely packed porous medium is used and rigid–rigid boundary condition is also being considered. Considering velocity, temperature, density and pressure fields in the quiescent basic state to be:

$$\left.\begin{aligned}
\mathbf{q} = \mathbf{q}_b = (0, 0),\\
\Theta_l(z) = \Theta_{l_b}(z), \quad \Theta_s(z) = \Theta_{s_b}(z),\\
\rho(z) = \rho_b(z), \quad P(z) = P_b(z),
\end{aligned}\right\}, \tag{12}$$

subject to

$$\left.\begin{aligned}
&\Theta_{l_b}(z) = \Theta_{s_b}(z) = \Theta_0 + 1 \quad &\text{at } Z = -\frac{1}{2},\\
&\Theta_{l_b}(z) = \Theta_{s_b}(z) = \Theta_0 \quad &\text{at } Z = \frac{1}{2},
\end{aligned}\right\}, \tag{13}$$

we obtain the quiescent state solution for the temperature distributions, subjected to the boundary condition Eq. (13), in the form:

$$\Theta_{l_b}(z) = \Theta_0 + \left(\frac{1}{2} - Z\right), \tag{14}$$

$$\Theta_{s_b}(z) = \Theta_0 + \left(\frac{1}{2} - Z\right). \tag{15}$$

We now superimpose perturbation on the quiescent basic state quantities and so we write:

$$\mathbf{q} = \mathbf{q}_b + \mathbf{q}', \quad \Theta_l = \Theta_{l_b} + \Theta_l', \quad \Theta_s = \Theta_{s_b} + \Theta_s', \quad P = P_b + P', \tag{16}$$

where the primes indicate a perturbed quantity. Eliminating the pressure term in Eq. (8) and introducing the stream function, Ψ, as follows

$$U = \frac{\partial \Psi}{\partial Z}, \quad W = -\frac{\partial \Psi}{\partial X}, \tag{17}$$

the dimensionless form of the vorticity and heat transport equations can be obtained in the form

$$\frac{1}{Pr}\frac{\partial}{\partial \tau}(\nabla^2\Psi) = \Lambda\nabla^4\Psi - \sigma^2\nabla^2\Psi - Ra_l\frac{\partial \Theta_l}{\partial X}, \tag{18}$$

$$\frac{\partial \Theta_l}{\partial \tau} = -\frac{\partial \Psi}{\partial X} + \nabla^2\Theta_l + H(\Theta_s - \Theta_l) + \frac{\partial \Psi}{\partial X}\frac{\partial \Theta_l}{\partial Z} - \frac{\partial \Psi}{\partial Z}\frac{\partial \Theta_l}{\partial X}, \tag{19}$$

$$\Gamma\frac{\partial \Theta_s}{\partial \tau} = \nabla^2\Theta_s + \gamma H(\Theta_l - \Theta_s). \tag{20}$$

In terms of the Darcy–Rayleigh number, Eq. (18) may be written as:

$$\frac{1}{Va}\frac{\partial}{\partial \tau}(\nabla^2\Psi) = \frac{\Lambda}{\sigma^2}\nabla^4\Psi - \nabla^2\Psi - Ra_D\frac{\partial \Theta_l}{\partial X}, \tag{21}$$

where $Va = Pr\sigma^2$ is the Vadasz number.

3 Marginal Stability: Stationary Convection

Since the linearized version of Eqs. (18)–(20) is self-adjoint, the principle of exchange of stabilities is valid and hence we consider only stationary convection. We consider two boundary conditions in the present study:

i Rigid–rigid, isothermal boundaries,
ii Free–free, isothermal boundaries (recap from Postelnicu and Rees 2003).

3.1 Rigid–Rigid, Isothermal Boundaries

The boundary conditions in this case for solving Eqs. (18)–(20) are:

$$\left.\begin{aligned} \Psi = \frac{\partial \Psi}{\partial Z} = 0 \quad &\text{at } Z = \pm\frac{1}{2}, \\ \Theta_l = \Theta_s = 0 \quad &\text{at } Z = \pm\frac{1}{2}, \end{aligned}\right\}. \tag{22}$$

To study the linear stability, we use the linearized version of Eqs. (18)–(20). The principle of exchange of stabilities is valid in the problem as Eqs. (18)–(20) are self-adjoint and hence we seek the solutions of Eqs. (18)–(20) in the form

$$\left.\begin{aligned} \Psi(X, Z) &= A\sin(kX)C_f(Z), \\ \Theta_l(X, Z) &= B\cos(kX)\sin\left(\pi Z + \frac{\pi}{2}\right), \\ \Theta_s(X, Z) &= C\cos(kX)\sin\left(\pi Z + \frac{\pi}{2}\right), \end{aligned}\right\}, \tag{23}$$

where

$$C_f(Z) = \frac{\cosh(\mu_1 Z)}{\cosh\left(\frac{\mu_1}{2}\right)} - \frac{\cos(\mu_1 Z)}{\cos\left(\frac{\mu_1}{2}\right)}, \tag{24}$$

and μ_1 = 4.73004074 (see Chandrasekhar 1961)

Substituting Eq. (23) into the linearized version of Eqs. (18)–(20) and using orthogonal condition with eigenfunctions give us the following system of equations:

$$\begin{pmatrix} Q_e & kRa_l Q_3 & 0 \\ 2kQ_3 & \delta_H & -H \\ 0 & \gamma H & -\delta_1^2 \end{pmatrix} \begin{pmatrix} A \\ B \\ C \end{pmatrix} = \begin{pmatrix} 0 \\ 0 \\ 0 \end{pmatrix}. \tag{25}$$

For a non-trivial solution of the system of homogeneous equations (25), we require

$$Ra_l^{\mathrm{RR}} = \frac{(k^2+\pi^2)Q_e}{2k^2 Q_3^2}\left(1 + \frac{H}{k^2+\pi^2+\gamma H}\right), \tag{26}$$

where

$$Q_e = \left[\Lambda(k^4+\mu_1^4) + k^2\sigma^2\right] Q_1 + \left(2k^2\Lambda + \sigma^2\right) Q_2,$$
$$Q_1 = \frac{1}{\mu_1}\left(\frac{\mu_1 - \sin\mu_1}{1+\cos\mu_1} + \frac{\mu_1 - \sinh\mu_1}{1+\cos h\mu_1}\right), \quad Q_2 = \mu_1\left(\frac{\mu_1 + \sin\mu_1}{1+\cos\mu_1} - \frac{\mu_1 + \sinh\mu_1}{1+\cos h\mu_1}\right),$$
$$Q_3 = -\frac{4\pi\mu_1^2}{\pi^4 - \mu_1^4}, \quad \delta^2 = k^2+\pi^2, \quad \delta_H = k^2+\pi^2+H, \quad \delta_1^2 = k^2+\pi^2+\gamma H.$$

In Eq. (26), we note that the Rayleigh number is of $O(k^4)$ as $k \to \infty$. The critical Rayleigh number, Ra_{l_c}, depends on both H and γ, and so we concentrate on Ra_{l_c} as a function of H and γ.

Asymptotic Analysis for Small and Large Values of H

For small values of H, the critical Rayleigh number, Ra_{l_c}, of LTNE is slightly above the critical value for LTE case, which may be confirmed by minimizing the small H series expansion of Eq. (26) given by

$$Ra_l^{\mathrm{RR}} = \frac{\delta^2 Q_e}{2k^2 Q_3^2} + \frac{Q_e}{2k^2 Q_3^2} H - \frac{\gamma Q_e}{2k^2\delta^2 Q_3^2} H^2 + \cdots. \tag{27}$$

Setting $\dfrac{\partial Ra_l^{\mathrm{RR}}}{\partial k} = 0$, we get the following equation for minimizing Ra_l^{RR}:

$$\begin{aligned} &2\delta^4(2k^6\Lambda - \pi^2\Lambda\mu_1^4 + k^4(\pi^2\Lambda + \sigma^2))Q_1 + (2k^4\Lambda - \pi^2\sigma^2)Q_2 \\ &+2\delta^4[\Lambda(k^4 - \mu_1^4)Q_1 - \sigma^2 Q_2]H \\ &+2\gamma[\{\Lambda\mu_1^4(2k^2+\pi^2) - k^4(\pi^2\Lambda - \sigma^2)\}Q_1 \\ &+\{2k^4\Lambda + \sigma^2(2k^2+\pi^2)\}Q_2]H^2 + \cdots = 0. \end{aligned} \tag{28}$$

Similarly, expanding k in terms of H, we get

$$k = k_0 + k_1 H + k_2 H^2 + \cdots, \tag{29}$$

where k_0 is the critical wave number for the LTE case and is given by the expression:

$$k_0^2 = \frac{M^2 - M\Delta_1 + \Delta_1}{6\Lambda Q_1 \Delta_1}, \tag{30}$$

where

$$M = (\pi^2\Lambda + \sigma^2)Q_1 + 2\Lambda Q_2,$$

$$
\begin{aligned}
\Delta_1 &= \left(\sqrt{F_{11}^2 - M^6} - F_{11}\right)^{\frac{1}{3}}, \\
F_{11} &= \pi^6\Lambda^3 Q_1^3 + 3\pi^4\Lambda^2 Q_1^2 F_{01} - F_{01}^3 - F_{02}, \\
F_{01} &= \sigma^2 Q_1 + 2\Lambda Q_2, \\
F_{02} &= 3\pi^2\Lambda Q_1[(18\Lambda^2\mu_1^4 - \sigma^4)Q_1^2 + 14\Lambda\sigma^2 Q_1 Q_2 - 4\Lambda^2 Q_2^2].
\end{aligned}
$$

Substituting Eq. (29) into Eq. (28) and equating the coefficients of like powers of H, we can find the first two corrections to k_0, namely k_1 and k_2, as follows:

$$
\begin{aligned}
k_1 &= -\frac{(k_0^2+\pi^2)[\Lambda(k_0^4-\mu_1^4)Q_1 - \sigma^2 Q_2]}{\Delta_{32}}, \\
k_2 &= -\frac{\Delta_{33}}{\delta_0^2\Delta_{32}},
\end{aligned}
$$

where

$$
\begin{aligned}
\Delta_{33} &= [k_0^2(2k_1\ell 4 - k_0^2\mu_1^2\gamma)\Lambda + \ell_2\Lambda\mu_1^4 + k_0^2 2\ell_1\sigma^2]Q_1 + (2\ell_1\Lambda + \ell_2\sigma^2)Q_2, \\
\ell_1 &= k_0^2[2k_1^2(14k_0^4 + 15k_0^2\mu_1^2 + 3\mu_1^4) + k_0^2\gamma], \\
\ell_2 &= (2k_0^2+\mu_1^2)\gamma - 2k_1[2k_0^3 + k_0(2+3k_0k_1)\mu_1^2 + k_1\mu_1^4], \\
\ell_3 &= 4k_0^4\Lambda + 2k_0^2\pi^2\Lambda - \pi^2\sigma^2, \\
\ell_4 &= k_0^5(4+45k_0k_1) + 2k_0^3(3+35k_0k_1)\mu_1^2 + 2k_0(1+15k_0k_1)\mu_1^4 + 3k_1\mu_1^6, \\
\Delta_{32} &= 4k_0[\{5k_0^6\Lambda - \pi^2\Lambda\mu_1^4 + k_0^2\pi^2(\pi^2\Lambda+\sigma^2) + k_0^4(5\pi^2\Lambda + 2\sigma^2)\}Q_1 + \ell_3 Q_2].
\end{aligned}
$$

For large values of H, Ra_l^{RR} takes the form

$$
Ra_l^{\mathrm{RR}} = \frac{\delta^2(\gamma+1)Q_e}{2\gamma k^2 Q_3^2} - \frac{\delta^4 Q_e}{2k^2\gamma^2 Q_3^2}\frac{1}{H} + \frac{\delta^6 Q_e}{2k^2\gamma^3 Q_3^2}\frac{1}{H^2} + \cdots \tag{31}
$$

Setting $\dfrac{\partial Ra_l^{\mathrm{RR}}}{\partial k} = 0$, we get the following expression:

$$
\begin{aligned}
&\gamma^2(1+\gamma)[(2k^6\Lambda - \pi^2\ \Lambda\mu_1^4 + k^4(\pi^2\Lambda+\sigma^2))Q_1 + (2k^4\Lambda - \pi^2\sigma^2)Q_2] \\
&\quad - \delta^2\gamma[\{3k^6\Lambda + \Lambda\mu_1^4(k^2-\pi^2) + k^4(\pi^2\Lambda + 2\sigma^2)\}Q_1 + \{4k^4\Lambda + \sigma^2(k^2-\pi^2)\}Q_2]\frac{1}{H} \\
&\quad + \delta^4[(4k^6\Lambda + \Lambda\mu_1^4(2k^2-\pi^2) + k^4(\pi^2\Lambda + 3\sigma^2))Q_1 \\
&\quad + (6k^4\Lambda + \sigma^2(2k^2-\pi^2))Q_2]\frac{1}{H^2}\cdots = 0.
\end{aligned} \tag{32}
$$

Similarly expanding k in terms of reciprocals of H, we get

$$
k = k_0 + k_1\frac{1}{H} + k_2\frac{1}{H^2} + \cdots \tag{33}
$$

Substituting Eq. (33) into Eq. (32) and equating the coefficients of like powers of H, we can obtain k_0 which is the critical wave number for the LTE case and is given by Eq. (30). The first two corrections to k_0 are given by

$$
k_1 = \frac{\Delta_{35}}{\Delta_{34}}, \quad k_2 = -\frac{\Delta_{36}}{\gamma\Delta_{34}}, \tag{34}
$$

where

$$
\begin{aligned}
\Delta_{34} &= 4k_0^3\gamma(1+\gamma)((3k_0^2\Lambda+\ \pi^2\Lambda+\sigma^2)Q_1+2\Lambda Q_2),\\
\Delta_{35} &= \delta_0^2[\{\Lambda(3k_0^6+(k_0^2-\pi^2)\mu_1^4)+k_0^4(\pi^2\Lambda+2\sigma^2)\}Q_1+\{4k_0^4\Lambda+(k_0^2-\pi^2)\sigma^2\}Q_2],\\
\Delta_{36} &= 4k_0^{10}\Lambda-24k_0^7k_1\gamma\Lambda-\pi^6\Lambda\mu_1^4+6k_0^2k_1^2\gamma^2(1+\gamma)(\pi^2\Lambda\ +\sigma^2)\\
&\quad -12k_0^5k_1\gamma(2\pi^2\Lambda+\sigma^2)+3k_0^8(3\pi^2\Lambda+\sigma^2)\\
&\quad -4k_0^3k_1\gamma(\Lambda(\pi^4+\mu_1^4)+2\pi^2\sigma^2)+2k_0^6(3\pi^4\Lambda+\Lambda\mu_1^4+3\pi^2\sigma^2)\\
&\quad +k_0^4(\Lambda(\pi^6+30k_1^2\gamma^2(1+\gamma)+3\pi^2\mu_1^4)+3\pi^4\sigma^2))Q_1\\
&\quad +[6k_0^8\Lambda-24k_0^5k_1\gamma\Lambda+12k_0^2k_1^2\gamma^2(1+\gamma)\Lambda-\ \pi^6\sigma^2\\
&\quad +3k_0^4\pi^2(2\pi^2\Lambda+\sigma^2)-4k_0^3k_1\gamma(4\pi^2\Lambda+\sigma^2)+2k_0^6(6\pi^2\Lambda+\sigma^2)]Q_2,
\end{aligned}
$$

and other quantities are as defined earlier.

3.2 Free–free, Isothermal Boundaries (Postelnicu and Rees 2003)

The boundary conditions for solving Eqs. (18)–(20) are:

$$
\left.\begin{aligned}
\Psi = \frac{\partial^2\Psi}{\partial Z^2} = 0 \quad \text{on } Z=\pm\frac{1}{2},\\
\Theta_l = \Theta_s = 0 \quad \text{on } Z=\pm\frac{1}{2},
\end{aligned}\right\}. \tag{35}
$$

We seek the solutions of Eqs. (18)–(20) in the form

$$
\left.\begin{aligned}
\Psi(X,Z) &= A\sin(kX)\sin\left(\pi Z+\frac{\pi}{2}\right),\\
\Theta_l(X,Z) &= B\cos(kX)\sin\left(\pi Z+\frac{\pi}{2}\right),\\
\Theta_s(X,Z) &= C\cos(kX)\sin\left(\pi Z+\frac{\pi}{2}\right),
\end{aligned}\right\}. \tag{36}
$$

Following the procedure used in Sect. 3.1, we get

$$
Ra_l^{\mathrm{FF}} = \frac{(k^2+\pi^2)^2\left[(k^2+\pi^2)\Lambda+\sigma^2\right]}{k^2}\left(1+\frac{H}{k^2+\pi^2+\gamma H}\right). \tag{37}
$$

The asymptotic analysis for small and large values of H is reported in Postelnicu and Rees (2003).

4 Weakly Nonlinear Stability Analysis for Steady and Finite Amplitude Convection

4.1 Rigid–Rigid, Isothermal Boundaries

A minimal double Fourier series which describes steady finite amplitude convection in a Newtonian liquid-saturated porous medium is given by

$$\left.\begin{aligned} \Psi(X,Z) &= \frac{1}{2\sqrt{\pi k}Q_4}A_1\sin(kX)C_f(Z),\\ \Theta_l(X,Z) &= -N_1\left(\frac{\sqrt{k}}{\sqrt{\pi}}B_1\cos(kX)\sin\left(\pi Z+\frac{\pi}{2}\right)-D_1\sin(2\pi Z+\pi)\right),\\ \Theta_s(X,Z) &= -N_1\left(N_2C_1\cos(kX)\sin\left(\pi Z+\frac{\pi}{2}\right)-N_3C_2\sin(2\pi Z+\pi)\right), \end{aligned}\right\}, \tag{38}$$

where

$$N_1=\frac{Q_3}{Fe_2Q_4r},\quad N_2=\frac{\gamma H\sqrt{k}}{(\delta^2+\gamma H)\sqrt{\pi}},$$
$$N_3=\frac{\gamma H}{4\pi^2+\gamma H},\quad Q_4=\frac{8\pi^2\mu_1^2\left(\mu_1^4+39\pi^4\right)}{\mu_1^8-82\pi^4\mu_1^4+81\pi^8}.$$

Substituting Eq. (38) into Eqs. (18)–(20) and using orthogonalization procedure of the Galerkin technique, the following Lorenz model is obtained:

$$\left.\begin{aligned} \frac{1}{Pr}\frac{dA_1}{d\tau} &= B_1-(Fe_1\Lambda+\sigma^2)A_1,\\ \frac{dB_1}{d\tau} &= A_1(Fe_2r-D_1)-(\delta^2+H)B_1+\frac{\gamma H^2}{\delta^2+H}C_1,\\ \frac{dD_1}{d\tau} &= -(4\pi^2+H)D_1+\frac{\gamma H^2}{4\pi^2+\gamma H}E_1+A_1B_1,\\ \Gamma\frac{dC_1}{d\tau} &= (\delta^2+H)(B_1-C_1),\\ \Gamma\frac{dE_1}{d\tau} &= (4\pi^2+H)(D_1-E_1), \end{aligned}\right\}, \tag{39}$$

where

$$r=\frac{Ra_l}{(Ra_l)_c},\quad Fe_1=\frac{Q_1(k^4+\mu_1^4)+2Q_2k^2}{Q_1k^2+Q_2},\quad Fe_2=\frac{(Ra_l)_cQ_3^2k^2}{\left(Q_1k^2+Q_2\right)}.$$

In “Appendix,” the derivation of the Ginzburg–Landau equation from Lorenz model Eq. (39) is presented, using the method of multiscales, leading us to believe that the weakly nonlinear analysis pursued in the paper is a properly defined one. Solving Eq. (39), we get the amplitudes of steady convection as follows

$$A_1^2=\frac{\delta^2(4\pi^2+H+\gamma H)\left(\delta^2+H+\gamma H\right)}{4\pi^2(4\pi^2+\gamma H)\left(\delta^2+\gamma H\right)}(r-1), \tag{40}$$

$$B_1=C_1=\frac{Fe_2\left(\delta^2+\gamma H\right)}{\delta^2\left(\delta^2+H+\gamma H\right)}A_1, \tag{41}$$

$$D_1 = E_1 = Fe_2(r-1). \tag{42}$$

The Nusselt number is defined as

$$Nu = \frac{\text{Amount of heat transfer by (conduction + convection)}}{\text{Amount of heat transfer by conduction}}.$$

Using Fourier law for the conductive and convective fluxes, we may write

$$Nu_l = 1 + \frac{\left[-\kappa_l \int_0^{\frac{2\pi}{k}} \frac{\partial \Theta_l}{\partial Z} \mathrm{d}X\right]_{Z=-\frac{1}{2}}}{\left[-\kappa_l \int_0^{\frac{2\pi}{k}} \frac{\mathrm{d}\Theta_{l_b}}{\mathrm{d}Z} \mathrm{d}X\right]_{Z=-\frac{1}{2}}}, \tag{43}$$

$$Nu_s = 1 + \frac{\left[-\kappa_s \int_0^{\frac{2\pi}{k}} \frac{\partial \Theta_s}{\partial Z} \mathrm{d}X\right]_{Z=-\frac{1}{2}}}{\left[-\kappa_s \int_0^{\frac{2\pi}{k}} \frac{\mathrm{d}\Theta_{s_b}}{bZ} \mathrm{d}X\right]_{Z=-\frac{1}{2}}}, \tag{44}$$

where Nu_l is Nusselt number of the liquid phase, Nu_s is that of the solid phase, $\Theta_{lb} = \dfrac{T_{lb}}{\Delta T}$ and $\Theta_{sb} = \dfrac{T_{sb}}{\Delta T}$.

The weighted average Nusselt number, Nu_w, for stationary mode of convection, evaluated at lower boundary $Z = -\dfrac{1}{2}$ for a single wavelength, is given by

$$Nu_w = \phi Nu_l + (1-\phi) Nu_s. \tag{45}$$

Substituting Eqs. (14)–(15) and Eq. (38) in Eqs. (43) and (44) and completing the integration, we get

$$Nu_l = 1 + 2\pi N_1 D_1, \tag{46}$$

$$Nu_s = 1 + 2\pi \frac{\gamma H}{4\pi^2 + \gamma H} N_1 E_1. \tag{47}$$

Using Eq. (42) in Eqs. (46) and (47), we get

$$Nu_l = 1 + 2\pi \frac{Q_3}{Q_4}\left(1 - \frac{1}{r}\right), \tag{48}$$

$$Nu_s = 1 + 2\pi \frac{\gamma H}{4\pi^2 + \gamma H} \frac{Q_3}{Q_4}\left(1 - \frac{1}{r}\right). \tag{49}$$

Substituting Eqs. (48) and (49) in Eq. (45), we get

$$Nu_w^{\mathrm{RR}} = 1 + 2\pi \left(\frac{4\pi^2\phi + \gamma H}{4\pi^2 + \gamma H}\right) \frac{Q_3}{Q_4}\left(1 - \frac{1}{r}\right). \tag{50}$$

Asymptotic Analysis for Small and Large Values of *H*

For small values of H with Ra_l^{RR} given by Eq. (27) and k_1 given by Eq. (29), Nu_w^{RR} takes the form

$$Nu_w^{\mathrm{RR}} = G_{11} + G_{21} H + G_{31} H^2 + \cdots, \tag{51}$$

where

$$
\begin{aligned}
G_{11} &= 1 + 2\phi \frac{Q_3}{Q_4}(1 - L_{12}),\\
G_{21} &= \frac{\gamma(1-\phi)(1-L_{12})Q_3}{2\pi^2 Q_4}\\
&\quad - \frac{L_{11}\phi Q_1 + [2k_0^3(1+2k_0k_1)\Lambda + (k_0 - 2k_1\pi^2)\sigma^2]\phi Q_2}{k_0^3 Ra_l Q_3 Q_4},\\
G_{31} &= \frac{2\gamma(1-\phi)}{32k_0^3\pi^4 Ra_l Q_3 Q_4}\{[k_0^4\{k_0(k_0^2+\pi^2)\gamma - 4\pi^2(k_0 + 4k_0^2k_1 + 2k_1\pi^2)\}\Lambda\\
&\quad + L_{13}\Lambda\mu^4 + L_{14}\sigma^2]Q_1 + (2L_{14}\Lambda + L13\sigma^2)Q_2 - 2k_0^3 Ra_l\gamma Q_3^2\}\\
&\quad - \frac{1}{k_0^4(k_0^2+\pi^2)Ra_l Q_3^2}\phi[\{k_0^4[(k_0^2+\pi^2)(2k_0(k_1 + 3k_0k_1^2 + 2k_0^2k_2)\\
&\quad + (k_1^2 + 2k_0k_2)\pi^2] - k_0^2\gamma)\Lambda - L_{15}\Lambda\mu^4 + L_{16}\sigma^2\}Q_1 + (2L_{16}\Lambda - L_{15}\sigma^2)Q_2],\\
L_{11} &= (k_0^4(k_0 + 4k_0^2k_1 + 2k_1\pi^2)\Lambda + (k_0 - 2k_1\pi^2)\Lambda\mu^4 + k_0^3(1+2k_0k_1)\sigma^2),\\
L_{12} &= (k_0^2+\pi^2)[\{\Lambda\,(k_0^4+\mu^4) + k_0^2\sigma^2\}Q_1 + (2k_0^2\Lambda + \sigma^2)Q_2]/2k_0^2 Ra_l Q_3^2,\\
L_{13} &= (8k_1\pi^4 + k_0\pi^2(\gamma - 4) + k_0^3\gamma), \quad L_{14} = k_0^3(k_0^2\gamma + \pi^2(\gamma - 8k_0k_1 - 4)),\\
L_{15} &= (k_0^2+\pi^2)[2k_0(k_1 + k_2\pi^2)] + k_0^2\gamma - 3k_1^2\pi^2,\\
L_{16} &= k_0^4[(k_1^2 + 2k_0k_2)(k_0^2+\pi^2) - \gamma].
\end{aligned}
$$

For large values of H, using Ra_l^{RR} given by Eq. (31) and k_1 given by Eq. (33), Nu_w^{rmRR} takes the form

$$
Nu_w^{\mathrm{RR}} = G_{41} + G_{51}H^{-1} + G_{61}H^{-2} + \cdots, \tag{52}
$$

where

$$
\begin{aligned}
G_{41} &= 3 - \frac{(k_0^2+\pi^2)(1+\gamma)[\{\Lambda(k_0^4+\mu^4) + k_0^2\sigma^2\}Q_1 + (2k_0^2\Lambda + \sigma^2)Q_2]}{k_0^2 Ra_l\gamma Q_3^2},\\
G_{51} &= [\{k_0^9\Lambda - \gamma(1+\gamma)[4k_0^6k_1\Lambda - 2k_1\pi^2\Lambda\mu^4 + 2k_0^4k_1(\pi^2\Lambda + \sigma^2)] + k_0\pi^4\Lambda\mu^4 L_{21}\\
&\quad + k_0^7(\sigma^2 + 2\pi^2\Lambda L_{24}) + k_0^3\pi^2(\pi^2\sigma^2 L_{21} + 2\Lambda\mu^4 L_{24})\\
&\quad + k_0^5(\Lambda\mu^4 + \pi^4\Lambda L_{21} + 2\pi^2\sigma^2 L_{24})\}Q_1 + [2k_0^7\Lambda - k_1\gamma(1+\gamma)(4k_0^4\Lambda - 2\pi^2\sigma^2)\\
&\quad + k_0\pi^4\sigma^2 L_{21} + k_0^5(\sigma^2 + 4\pi^2\Lambda L_{24}) + 2k_0^3\pi^2(\pi^2\Lambda L_{21} + \sigma^2 L_{24})]Q_2\\
&\quad + 8k_0^3\pi^2 Ra_l\gamma(\phi - 1)Q_3^2)]/k_0^3 Ra_l\gamma^2 Q_3^2,\\
G_{61} &= -[\{k_0^{12}\Lambda - 6k_0^9k_1\gamma\Lambda + 3k_1^2\pi^2\gamma^2(1+\gamma)\Lambda\mu^4 + k_0^{10}(\sigma^2 + \pi^2\Lambda(7-4\phi))\\
&\quad + k_0^2\pi^6\Lambda\mu^4 L_{23} - 2k_0\pi^2\gamma\Lambda\mu^4(k_2\gamma(1+\gamma) - k_1\pi^2 L_{21})\\
&\quad + k_0^8(\Lambda\mu^4 + \pi^2\sigma^2(7-4\phi) + \pi^4\Lambda L_{22}) + k_0^6\{6k_1^2\gamma^2(1+\gamma)\Lambda + \pi^2\Lambda\mu^4(7-4\phi)\\
&\quad + \pi^4\sigma^2 L_{22} + \pi^6\Lambda L_{23}\} + 4k_0^7\gamma(k_2\gamma(1+\gamma)\Lambda - k_1(\sigma^2 + 2\pi^2\Lambda L_{24}))\\
&\quad + 2k_0^5\gamma(k_2\gamma(1+\gamma)(\pi^2\Lambda + \sigma^2) - k_1(\Lambda\mu^4 + 2\pi^2\sigma^2 L_{24} + \pi^4\Lambda L_{21}))\\
&\quad + k_0^4(k_1^2\gamma^2(1+\gamma)(\pi^2\Lambda + \sigma^2) + \pi^4(\Lambda\mu^4 L_{22} + \pi^2\sigma^2 L_{23}))\}Q_1\\
&\quad + [2k_0^{10}\Lambda - 8k_0^7k_1\gamma\Lambda + 3k_1^2\pi^2\gamma^2(1+\gamma)\sigma^2 + k_0^8(\sigma^2 + 2\pi^2\Lambda(7-4\phi))\\
&\quad + k_0^2\pi^6\sigma^2 L_{23} - 2k_0\pi^2\gamma\sigma^2(k_2\gamma(1+\gamma) - k_1\pi^2 L_{21})\\
&\quad + k_0^6\pi^2(\sigma^2(7-4\phi) + 2\pi^2\Lambda L_{22})
\end{aligned}
$$

$$+k_0^4(2k_1^2\gamma^2(1+\gamma)\Lambda+\pi^4\sigma^2 L_{22}+2\pi^6\Lambda L_{23})+2k_0^5\gamma\{2k_2\gamma(1+\gamma)\Lambda$$
$$-k_1(\sigma^2+4\pi^2\Lambda L_{24})\}]Q_2]/k_0^4 Ra_l\gamma^3 Q_3^2+32\pi^4\gamma^{-2}(\phi-1),$$

$$L_{21}=5+4\gamma-4(1+\gamma)\phi,\ L_{22}=27+16\gamma-8(3+2\gamma)\phi,$$
$$L_{23}=21+16\gamma-4(5+4\gamma)\phi,\ L_{24}=3+2\gamma-2(1+\gamma)\phi.$$

4.2 Free–Free, Isothermal Boundaries

A minimal double Fourier series which describes steady finite amplitude convection is given by

$$\left.\begin{aligned}\Psi(X,Z)&=\frac{1}{\sqrt{\pi k\pi}}A_2\sin(kX)\sin\left(\pi Z+\frac{\pi}{2}\right),\\ \Theta_l(X,Z)&=-N_1\left(\frac{\sqrt{k}}{\sqrt{\pi}}B_2\cos(kX)\sin\left(\pi Z+\frac{\pi}{2}\right)-D_2\sin\left(2\pi Z+\pi\right)\right),\\ \Theta_s(X,Z)&=-N_1\left(N_2C_2\cos(kX)\sin\left(\pi Z+\frac{\pi}{2}\right)-N_3E_2\sin\left(2\pi Z+\pi\right)\right),\end{aligned}\right\},\tag{53}$$

where

$$N_1=-\frac{1}{Fe_2\pi r}.$$

Following the procedure of Sect. 4.1 and substituting Eq. (53) into Eqs. (18)–(20) , we get Eq. (39) but with certain quantities redefined as follows

$$Fe_1=k^2+\pi^2,\quad Fe_2=\frac{(Ra_l)_c\pi^4k^2}{2\delta^2}.$$

Solving Eq. (39) with the above redefined quantities, we get the amplitudes of steady-state convection as follows:

$$A_2^2=\frac{\delta^2(4\pi^2+H+\gamma H)\left(\delta^2+H+\gamma H\right)}{4\pi^2(4\pi^2+\gamma H)\left(\delta^2+\gamma H\right)}(r-1),\tag{54}$$

$$B_2=C_2=\frac{Fe_2\left(\delta^2+\gamma H\right)}{\delta^2\left(\delta^2+H+\gamma H\right)}A,\tag{55}$$

$$D_2=E_2=Fe_2(r-1).\tag{56}$$

Substituting Eqs. (14)–(15) and (53) in Eqs. (43) and (44) and completing the integration, we get

$$Nu_l=1-2\pi N_1D_3,\tag{57}$$
$$Nu_s=1-2\pi N_1N_3E_3.\tag{58}$$

Following the procedure of Sect. 4.1, we get the liquid, solid and weighted average Nusselt numbers in the form:

$$Nu_l=1+2\left(1-\frac{1}{r}\right),\tag{59}$$

$$Nu_s=1+2\frac{\gamma H}{(4\pi^2+\gamma H)}\left(1-\frac{1}{r}\right),\tag{60}$$

$$Nu_w^{\mathrm{FF}}=1+2\left(\frac{4\pi^2\phi+\gamma H}{4\pi^2+\gamma H}\right)\left(1-\frac{1}{r}\right).\tag{61}$$

Asymptotic Analysis of Nu_w for Small and Large Values of H

For small values of H, using $Ra_{l_c}^{\mathrm{FF}}$ given by Eq. (37), Nu_w^{FF} given by Eq. (61) takes the form

$$Nu_w^{\mathrm{FF}} = G_{13} + G_{23}H + G_{33}H^2 + \cdots, \tag{62}$$

where

$$G_{13} = \frac{k_0^2 Ra_l - 2\zeta\phi}{k_0^2 Ra_l}, \quad G_{23} = \frac{k_0\gamma\zeta - 2\pi^2\zeta_1\phi}{2k_0^3\pi^2 Ra_l},$$

$$G_{33} = \frac{(k_0\gamma^2\zeta - 4\pi^2\gamma\zeta_1)(1-\phi)}{8k_0^3\pi^4 Ra_l} - \frac{2\zeta_2\phi}{k_0^4 Ra_l},$$

$$\zeta = -k_0^2 Ra_l + k_0^6\Lambda + 3k_0^4\pi^2\Lambda + 3k_0^2\pi^4\Lambda + \pi^6\Lambda + (k_0^2+\pi^2)^2\sigma^2,$$

$$\zeta_1 = (k_0^2+\pi^2)[(k_0 + 2k_0^2k_1 - 2k_1\pi^2)\{(k_0^2+\pi^2)\Lambda + \sigma^2\} + 2k_0^2k_1(k_0^2+\pi^2)\Lambda],$$

$$\begin{aligned}\zeta_2 = &-6k_0^6k_1^2\Lambda - 4k_0^7k_2\Lambda + [2k_0\pi^2(k_1 + k_2\pi^2) - 3k_1^2\pi^4](\pi^2\Lambda + \sigma^2)\\ &+ k_0^2\gamma(\pi^2\Lambda+\sigma^2) + k_0^4[\gamma\Lambda - k_1^2(3\pi^2\Lambda+\sigma^2)] + 2k_0^5\{k_1\Lambda - k_2(3\pi^2\Lambda+\sigma^2)\}.\end{aligned}$$

For large values of H, with Ra_l^{FF} given by Eq. (37) and k from Postelnicu and Rees (2003), Nu_w^{FF} takes the form

$$Nu_w^{\mathrm{FF}} = G_{43} + G_{53}H^{-1} + G_{63}H^{-2} + \cdots, \tag{63}$$

where

$$G_{43} = 1 + 2\left(1 - [(k_0^2+\pi^2)^2(1+\gamma)[(k_0^2+\pi^2)\,\Lambda + \sigma^2]]/k_0^2 Ra_l\gamma\right),$$

$$\begin{aligned}G_{53} = 2\{&k_0^9\Lambda - \gamma(1+\gamma)[4k_0^6k_1\Lambda - 2k_1\pi^4(\pi^2\Lambda+\sigma^2) + 2k_0^4k_1(3\pi^2\Lambda+\sigma^2)]\\ &- k_0\pi^6(\pi^2\Lambda+\sigma^2)L_{61} + k_0^7L_{63} + k_0^5\pi^2(\sigma^2L_{63} - 6\pi^2\Lambda L_{64})\\ &+ k_0^3\pi^2[16\pi^4\Lambda + 4Ra_l\gamma(\phi+1) + \pi^2(11\sigma^2 + 4(3\pi^2\Lambda + 2\sigma^2)\\ &(\gamma - (1+\gamma)\phi))]\}/k_0^3 Ra_l\gamma^2,\end{aligned}$$

$$\begin{aligned}G_{63} = -2[&k_0^{12}\Lambda - 6k_0^9k_1\gamma\Lambda + 3k_1^2\pi^4\gamma^2(1+\gamma)(\pi^2\,\Lambda+\sigma^2)\\ &+ k_0^{10}(\sigma^2 + \pi^2\Lambda(9-4\phi)) - k_0^2\pi^8(\pi^2\Lambda+\sigma^2)L_{60} + k_0^4[3k_1^2\pi^2\gamma^2\Lambda\\ &+ k_1^2\gamma^2\sigma^2 + \pi^8\Lambda L_{69} + 16\pi^4 Ra_l\gamma(\phi+1) + 4\pi^6\sigma^2L_{68}]\\ &- 2k_0\pi^4\gamma(\pi^2\Lambda+\sigma^2)(k_2\,\gamma(1+\gamma) - k_1\pi^2L_{21}) + 2k_0^8\pi^2(2\sigma^2(2-\phi) + \pi^2\Lambda L_{65})\\ &+ 2k_0^6(3k_1^2\gamma^2\Lambda + \pi^6\Lambda L_{66} + \pi^4\sigma^2L_{67}) + 4k_0^7\gamma(k_2\gamma\Lambda - k_1L_{62})\\ &+ 2k_0^5\gamma\{k_2\gamma(3\pi^2\Lambda+\sigma^2) - k_1\pi^2(6\pi^2\Lambda L_{64} + \sigma^2L_{63})\}]/k_0^4 Ra_l\gamma^3,\end{aligned}$$

$$L_{60} = 16\gamma(\phi-1) + 20\phi - 21,\ \ L_{61} = 4\phi - 5 + 4\gamma(\phi-1),$$

$$L_{62} = 4\pi^2\Lambda(\gamma(\phi-1) + \phi - 2) - \sigma^2,\ \ L_{63} = 7 + 4\gamma - 4(1+\gamma)\phi,$$

$$L_{64} = 3 + 2\gamma - 2(1+\gamma)\phi,\ \ L_{65} = 21 + 8\gamma - 8(2+\gamma)\phi,$$

$$L_{66} = 41 + 24\gamma - 12(3+2\gamma)\phi,\ \ L_{67} = 17 + 8\gamma - 2(7+4\gamma)\phi,$$

$$L_{68} = 12 + 8\gamma - 11\phi - 8\gamma\phi,\quad L_{69} = 69 - 48\gamma(\phi-1) - 64\phi.$$

5 Results and Discussion

Linear and weakly nonlinear analyses have been carried out for the Brinkman–Bénard problem with LTNE effects. Rigid–rigid and free–free, isothermal boundaries have been considered in the analyses. Equation (23) is not an exact solution of the linearized version of Eqs. (18)–(20), and hence, the critical wave number and Rayleigh number have been obtained by the shooting method to obtain them to an accuracy of 10^{-4}. This is documented in Table 1, which clearly shows that the maximum percentage error in k_c and Ra_{lc} between the Galerkin and shooting methods is 0.86 and 1.73%, respectively. These percentage errors are indicated in bold in Table 1. Linear theory result depicted in Fig. 2 reiterates the validity of the following classical result in the present problem:

$$Ra_{l_c}^{\mathrm{FF}} < Ra_{l_c}^{\mathrm{RR}}. \tag{64}$$

In addition to Fig. 2, we observe the following result:

$$Ra_{l_c}^{LTNE} < Ra_{l_c}^{LTE}. \tag{65}$$

Before we discuss the results of Fig. 2 further, we need to know that LTNE effect is important when one of the following conditions is true:

(a) $H \gg 0$,
(b) $\gamma \gg 0$.

One may also conclude that LTNE effect is important when

(c) $H \geq 1$ with γH fixed or
(d) H fixed and $\gamma H \gg 1$.

From the definitions of H and γ, it is quite clear that when ϕ is close to 1 we have $\gamma H \gg 1$ and when ϕ is close to 0 then H is large.

In Fig. 2, we also infer that the LTNE effect ceases when γ and/or H is quite large. In other words, when thermal conductivity of solid phase is very small in comparison with that of liquid phase, the medium does not allow the LTNE effect to be important. Table 2 gives us the exact meaning of $H \to 0$ and $H \to \infty$ for large values of γ. For example in the case of free–free boundaries with a value of 10 for γ, we see that $H \to 0$ would mean any value of H equal to or smaller than 0.072 and the same is presented in Fig. 3. Similarly, $H \to \infty$ would mean any value of H equal to or greater than 279.161, and this is presented in Fig. 4. In Table 2, it is evident that the exact meaning of $H \to 0$ and $H \to \infty$ predominantly depends on the values of γ and less predominantly on the type of velocity boundary condition.

On increasing the individual or collective values of Λ, σ^2 and H, the value of critical Rayleigh number increases, and there is thus a delay in the onset of convection which thereby leads to decrease in amount of heat transport, and the same is shown in Figs. 5, 6, 7 and 8. The effect of Λ is more significant than the effect of σ^2 on onset and more pronounced in rigid–rigid, isothermal boundary than in the case of free–free, isothermal boundary. The effect of increasing the value of γ is to advance the onset of convection and thereby increase the amount of heat transport. The effect is more significant for small values of γ, and its effect ceases for large values. This result is to be expected since LTNE effect is important only when γ is small. This is essentially a reiteration of what is conveyed by Eq. (65). From nonlinear theory, we may infer that

$$Nu_w^{\mathrm{FF}} > Nu_w^{\mathrm{RR}}.$$

Table 1 Comparison of critical wave number, k_c, and Rayleigh number, Ra_{lc}, obtained by shooting method (SM) and by using Chandrasekhar function (CF), ($E - \%$ error)

γ	$\log_{10} H$	Λ	σ^2	k_c (SM)	k_c (CF)	Ra_{lc} (SM)	Ra_{lc} (CF)	E in k_c	E in Ra_{lc}
1	0	1.0	00	3.164	3.1445	1789.8526	1812.2448	0.63	1.25
			05	3.184	3.1642	2021.8620	2051.0406	0.62	1.44
			10	3.200	3.1810	2252.9343	2289.6447	0.62	1.62
		1.5	00	3.164	3.1445	2684.7789	2718.3673	0.63	1.25
			05	3.177	3.1580	2916.7789	2957.1987	0.59	1.38
			10	3.189	3.1702	3148.4785	3195.8915	0.59	1.50
		2.0	00	3.164	3.1445	3579.7052	3624.4897	0.63	1.25
			05	3.174	3.1548	3811.9646	3863.3398	0.63	1.43
			10	3.184	3.1642	4043.72403	4102.0813	0.62	1.44
	2	1.0	00	3.201	3. 1798	3129.7032	3172.1055	0.63	1.35
			05	3.223	3.2019	3534.7226	3589.3190	0.68	1.54
			10	3.241	3.2208	3938.0806	4006.1333	0.65	**1.73**
		1.5	00	3.200	3.1798	4694.5548	4758.1583	0.66	1.35
			05	3.216	3.1949	5099.8682	5175.4458	0.68	1.48
			10	3.230	3.2085	5504.0231	5592.4452	0.68	1.61
		2.0	00	3.200	3.198	6259.4073	6344.2111	0.60	1.35
			05	3.212	3.1913	6664.8699	6761.5372	0.65	1.45
			10	3.223	3.2019	7069.4450	7178.6381	0.68	1.54
1	4	1.0	00	3.118	3.0986	3412.1250	3453.4105	0.64	1.21
			05	3.135	3.1165	3855.3881	3909.4656	0.61	1.40
			10	3.150	3.1317	4296.8871	4365.2137	0.60	1.59
		1.5	00	3.117	3.0985	5118.1868	5180.1158	0.61	1.21
			05	3.131	3.1108	5561.7640	5636.2280	0.67	1.34
			10	3.140	3.1218	6004.1102	6092.1180	0.61	1.47
		2.0	00	3.118	3.0985	6824.2489	6906.8211	0.64	1.21
			05	3.125	3.1079	7267.9814	7362.9631	0.66	1.31
			10	3.135	3.1165	7710.7779	7818.9312	0.61	1.40
1	6	1.0	00	3.117	3.0975	3415.4657	3456.7351	0.64	1.21
			05	3.128	3.1154	3859.1802	3913.2507	0.42	1.40
			10	3.149	3.1305	5301.0244	4369.4605	0.59	1.29
		1.5	00	3.120	3.0975	5123.1505	5185.1027	0.35	1.21
			05	3.128	3.1098	5567.1532	5641.6752	0.61	1.34
			10	3.146	3.1207	6009.8237	6098.0263	0.83	1.47
		2.0	00	3.116	3.0975	6830.8124	6913.4702	0.61	1.21
			05	3.114	3.1068	7275.0005	7370.0725	0.26	1.31
			10	3.142	3.1154	7718.2088	7826.5014	**0.86**	1.40

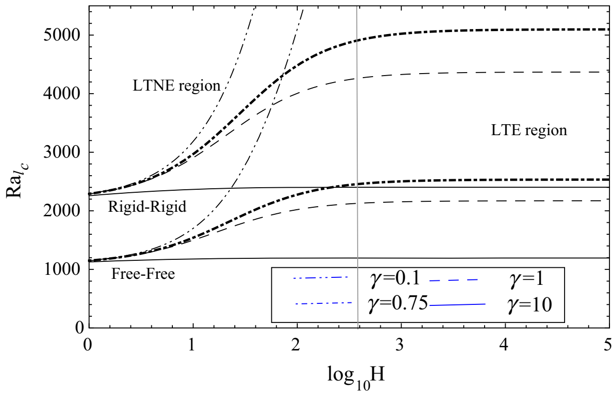

Fig. 2 Variation of critical value of Rayleigh number, Ra_{l_c}, with heat transfer coefficient, H, for different values of ratio of thermal conductivities, γ, and fixed value of Brinkman number, $\Lambda = 1$, and porous parameter, $\sigma^2 = 10$

Table 2 Exact meaning of $H \to 0$ and $H \to \infty$, for large values of γ , and $\Lambda = 1$ and $\sigma^2 = 5$

γ	Free–free		Rigid–rigid	
	$H \to 0$ (LTNE)	$H \to \infty$ (LTE)	$H \to 0$ (LTNE)	$H \to \infty$ (LTE)
010	0.072	279.161	0.147	250.965
020	0.030	139.997	0.057	126.715
030	0.019	093.424	0.036	084.750
040	0.014	070.102	0.026	063.665
050	0.011	056.098	0.021	050.980
060	0.009	046.758	0.017	042.510
070	0.008	040.084	0.014	036.455
080	0.007	035.077	0.012	031.910
090	0.006	031.182	0.011	028.375
100	0.005	028.066	0.010	025.540

Figure 9 demonstrates that the amount of heat transport in LTNE case is more than that in the case of LTE. We also recover the Nusselt number of classical LTE case by considering large values of H and by considering the mean properties of liquid and solid phases. In Figs. 5, 6, 7, 8 and 9, we note that the actual Rayleigh numbers chosen for plotting the graphs are greater than the critical Rayleigh number as it should be for the convective regime. It is to be noted here that the results in the figures concerning weakly nonlinear theory are valid in the region where values of Ra_l are close to the onset value Ra_{lc}. Thus, the values of the Nusselt number corresponding to $Ra_l > 2Ra_{lc}$ can be inaccurate for both rigid–rigid and free–free boundaries.

The following conclusions are drawn from the present study:

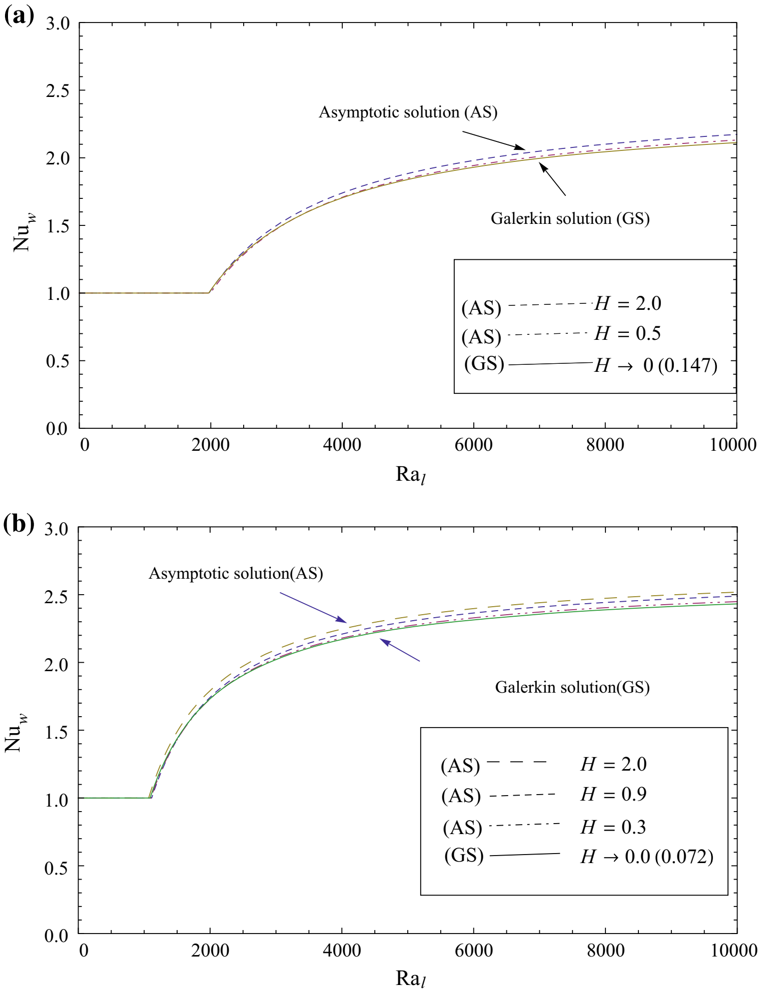

Fig. 3 Variation of weighted average Nusselt number, Nu_w, with Ra_l for $\Lambda = 1$, $\sigma^2 = 5$, $\gamma = 10$, for small values of H. **a** Rigid–rigid, isothermal boundary. **b** Free–free, isothermal boundary

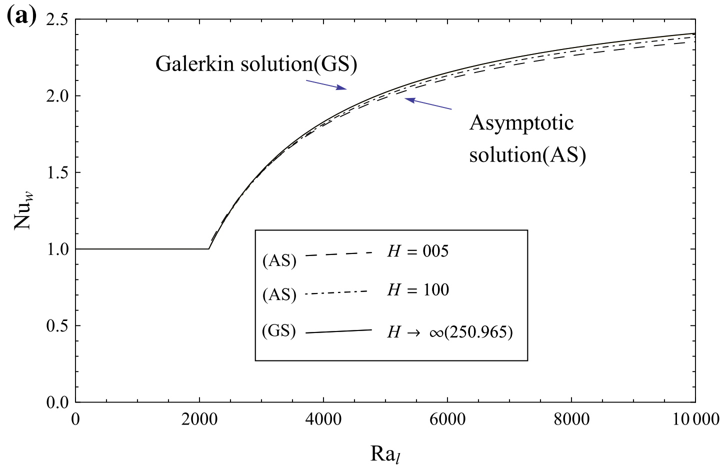

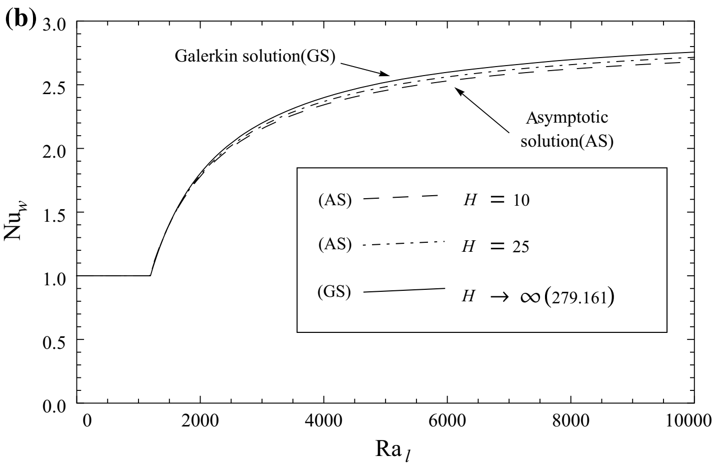

Fig. 4 Variation of Nu_w with Ra_l for $\Lambda = 1, \sigma^2 = 5, \gamma = 10$, for large values of H. **a** Rigid–rigid, isothermal boundary. **b** Free–free, isothermal boundary

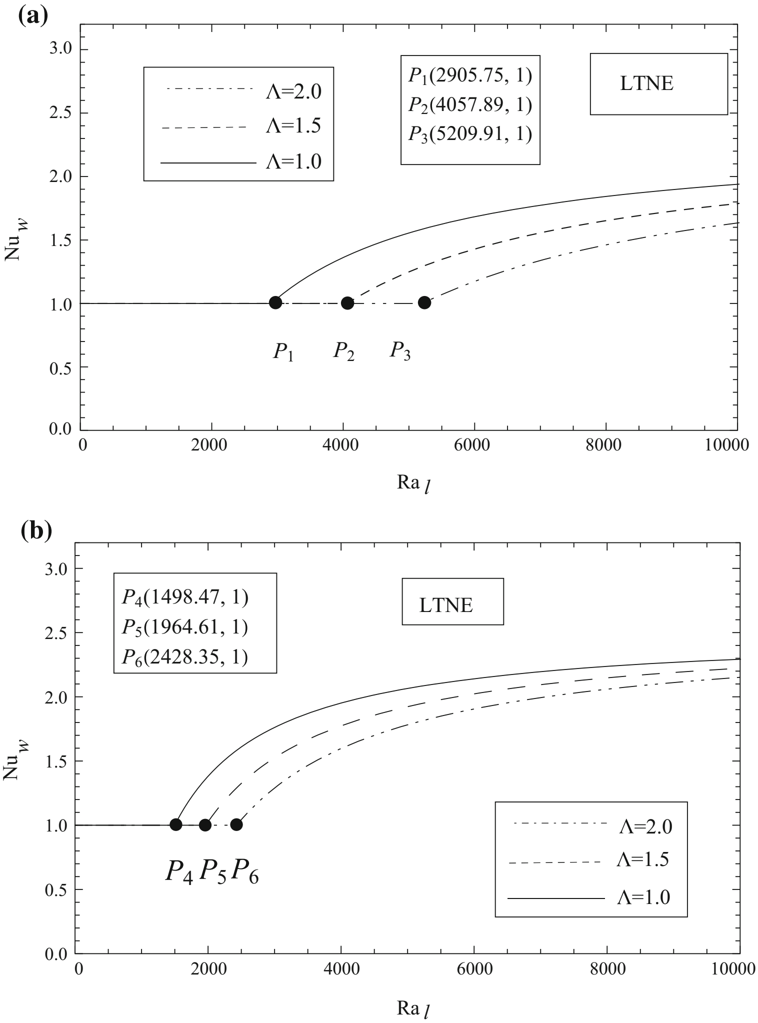

Fig. 5 Variation of Nu_w with Ra_l for different values of Λ, and for fixed value of $\sigma^2 = 10$, $H = 10$, and $\gamma = 1$. **a** Rigid–rigid, isothermal boundary. **b** Free–free, isothermal boundary

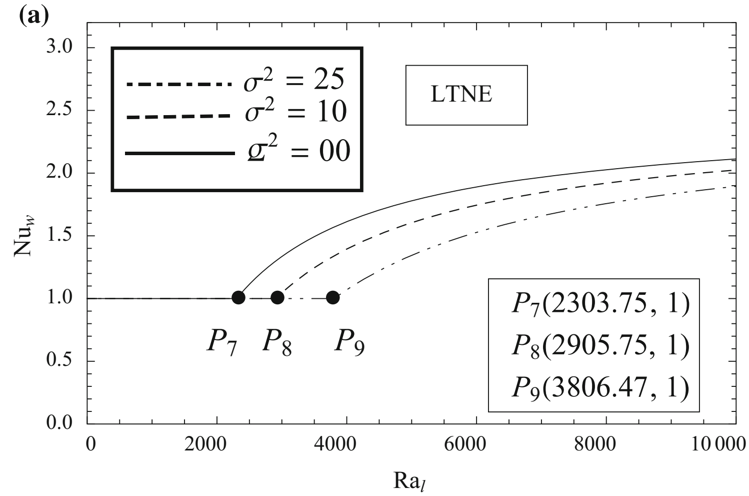

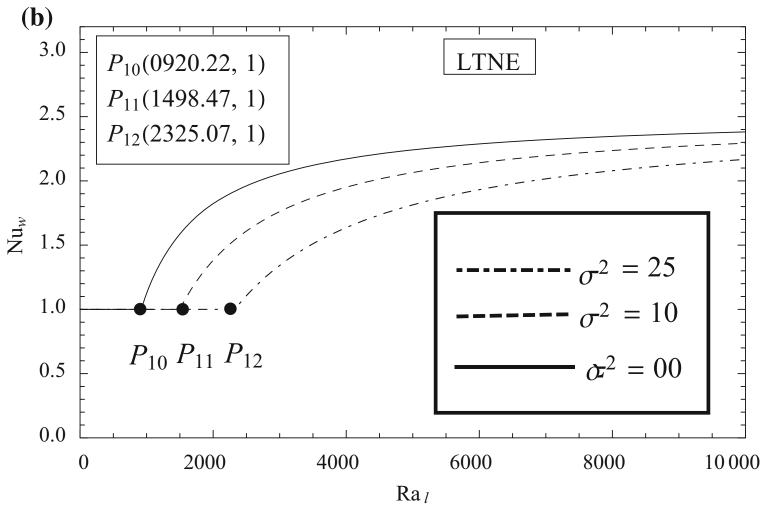

Fig. 6 Variation of Nu_w with Ra_l for different values of σ^2, and for fixed value of other parameters $\Lambda = 1$, $H = 10$, $\gamma = 1$. **a** Rigid–rigid, isothermal boundary. **b** Free–free, isothermal boundary

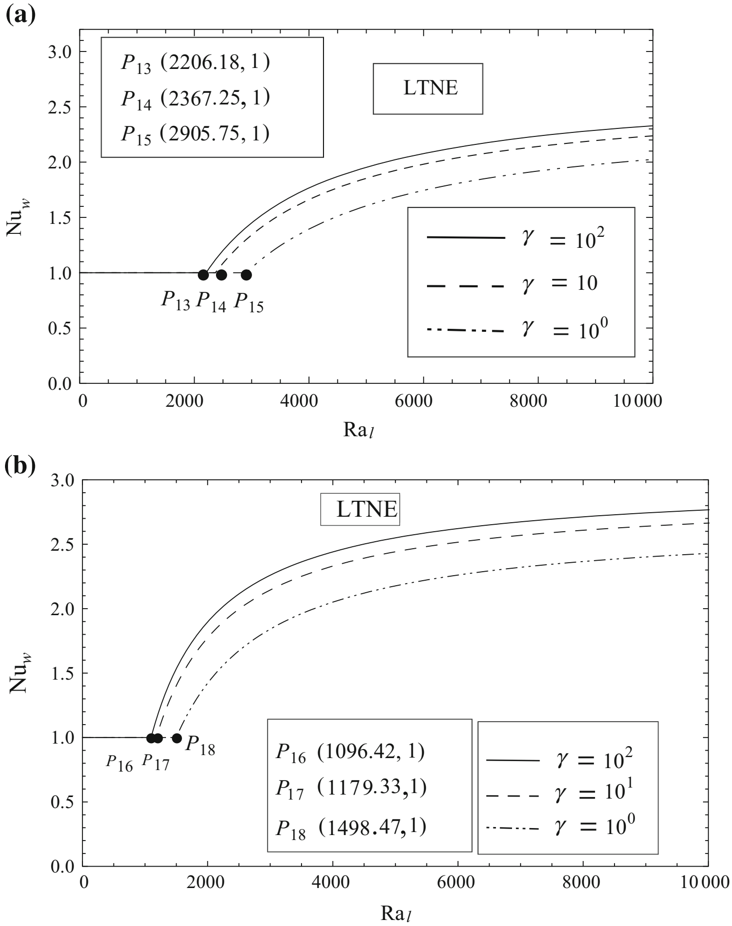

Fig. 7 Variation of Nu_w with Ra_l for different values of γ, and for fixed value of other parameters $H = 10$, $\sigma^2 = 10$, $\Lambda = 1$. **a** Rigid–rigid, isothermal boundary. **b** Free–free, isothermal boundary

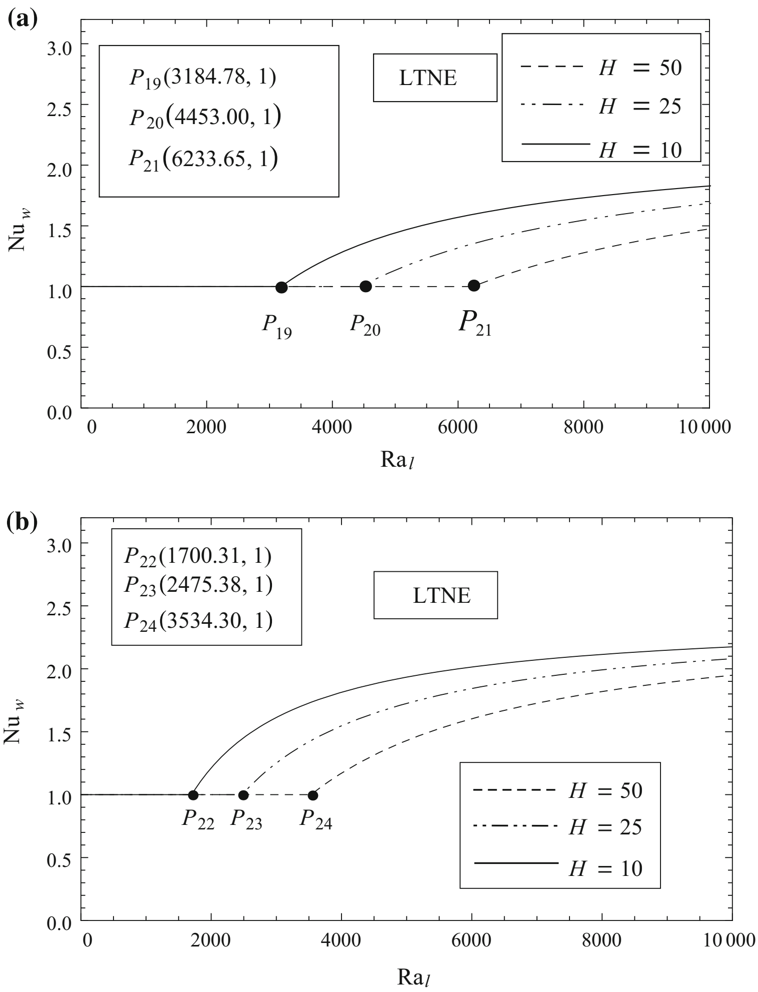

Fig. 8 Variation of Nu_w with Ra_l for different values of H, and for fixed value of other parameters $\gamma = 0.1$, $\sigma^2 = 10$, $\Lambda = 1$. **a** Rigid–rigid, isothermal boundary. **b** Free–free, isothermal boundary

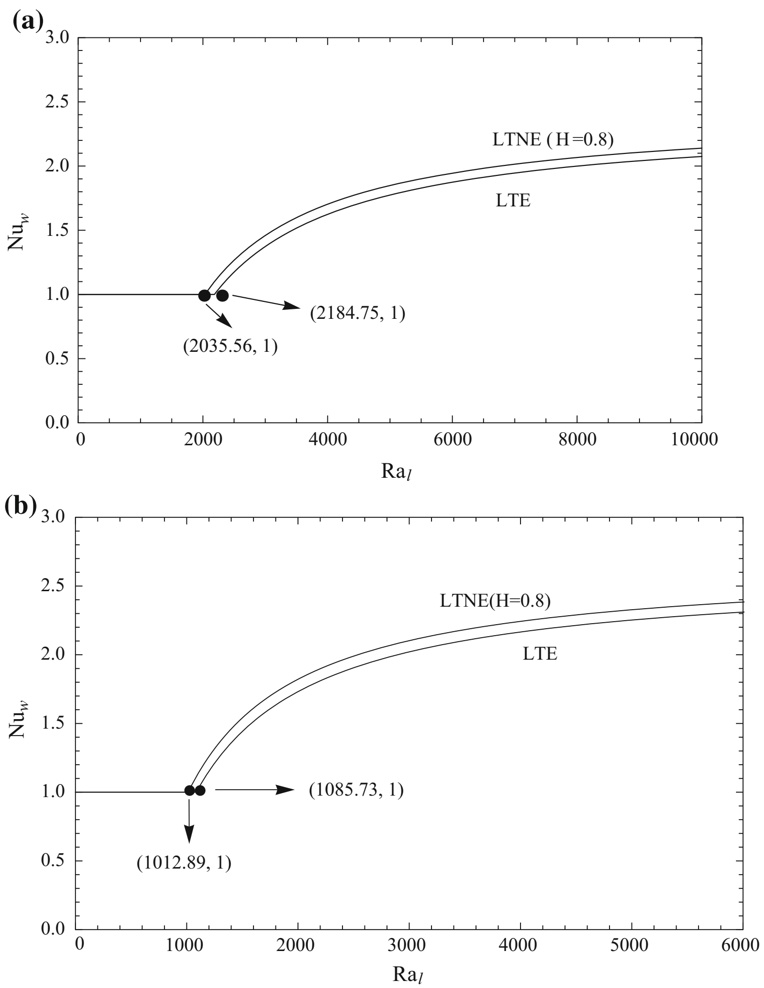

Fig. 9 Variation of Nu_w with Ra_l of LTNE and LTE for $\Lambda = 1, \quad \sigma^2 = 10, \quad \gamma = 1$. [This figure is to be seen in conjunction with Table 2.] **a** Rigid–rigid, isothermal boundary. **b** Free–free, isothermal boundary

6 Conclusions

(i) A highly accurate approximate solution with a percentage error of a maximum of 1.73% in the case of rigid–rigid, isothermal boundaries is possible by using Chandrasekhar function. A more accurate value for critical Rayleigh number than that of Postelnicu (2008) is obtained in this case.
(ii) The effect of increasing Λ, σ^2 and H is to stabilize the system, whereas increasing the values of γ is to destabilize the system.
(iii) It is observed that Rayleigh number, by considering mean values of thermophysical properties of liquid and solid phases, approaches a constant value of LTE case for large values of H.
(iv) Λ, σ^2, H, and γ have a significant effect on heat transport.

(v) The onset of convection is delayed in the case of rigid–rigid, isothermal boundaries than that in the case of free–free, isothermal boundaries. This leads to a 'diminished heat transport' situation in the case of the former boundary condition compared to the latter.
(vi) For large values of σ^2, the asymptotic values of Darcy–Rayleigh number and Nusselt number can be obtained for the two boundary combinations by considering Eq. (21). This would essentially mean using Va, $\frac{\Lambda}{\sigma^2}$ and Ra_D in place of Pr, Λ and Ra_l in Eqs. (26), (27), (31), (37), and the corresponding expressions taken from Sect. (4) for Nusselt numbers in the case of low-porosity medium.

Acknowledgements The authors are grateful to the referees for many useful comments which helped us to refine the paper to the present form.

Appendix

Derivation of Ginzburg–Landau Equation from the Lorenz Model by the Method of Multiscales (Siddheshwar and Kanchana 2017)

To use the method of multiscales, we expand the amplitudes in terms of the small quantity ε as follows:

$$\left.\begin{aligned} A &= \varepsilon A_1 + \varepsilon^2 A_2 + \varepsilon^3 A_3 + \cdots,\\ B_1 &= \varepsilon B_{11} + \varepsilon^2 B_{12} + \varepsilon^3 B_{13} + \cdots,\\ D_1 &= \varepsilon D_{11} + \varepsilon^2 D_{12} + \varepsilon^3 D_{13} + \cdots,\\ C_1 &= \varepsilon C_{11} + \varepsilon^2 C_{12} + \varepsilon^3 C_{13} + \cdots,\\ E_1 &= \varepsilon E_{11} + \varepsilon^2 E_{12} + \varepsilon^3 E_{13} + \cdots,\\ r &= 1 + \varepsilon^2 r_2, \end{aligned}\right\}, \tag{66}$$

and a slow time scale may also be introduced as follows:

$$\tau^* = \varepsilon^2 \tau. \tag{67}$$

Substituting Eqs. (66)–(67) in Eq. (39), equating the coefficients of like powers of ε on either side of the equation, we get
Coefficient of ε.

$$LM^{(1)} = 0, \tag{68}$$

where

$$L = \begin{pmatrix} -Fe_1\Lambda - \sigma^2 & 1 & 0 & 0 & 0 \\ Fe_2 & -\delta^2 - H & 0 & \dfrac{H^2\gamma}{\delta^2 + H\gamma} & 0 \\ 0 & 0 & -4\pi^2 - H & 0 & \dfrac{H^2\gamma}{4\pi^2 + H\gamma} \\ 0 & 1 & 0 & -1 & 0 \\ 0 & 0 & 1 & 0 & -1 \end{pmatrix},$$

$M^{(i)} = (A_i, B_{1i}, D_{1i}, C_{1i}, E_{1i})^{\mathrm{T}}, \quad (i = 1, 2, 3).$

Solving Eq. (68), we get the solution of the first-order system as follows:

$$B_{11} = C_{11} = \frac{\left(\gamma H + \delta^2\right) Fe_2 r_0}{\delta^2 \left(\delta^2 + H + \gamma H\right)} A_1, \quad D_{11} = E_{11} = 0. \tag{69}$$

Coefficient of ε^2

$$LM^{(2)} = [R_{21},\ R_{22},\ R_{23},\ R_{24},\ R_{25}]^{\mathrm{T}}, \tag{70}$$

where

$$R_{21} = 0, \quad R_{22} = 0, \ R_{23} = -\frac{\left(\gamma H + \delta^2\right) Fe_2 r_0}{\delta^2 \left(\gamma H + H + \delta^2\right)} A_1^2, \quad R_{24} = 0, \quad R_{25} = 0.$$

Solving Eq. (70), we get the solution of the second-order system as follows:

$$A_2 = B_{12} = C_{12} = 0, \quad D_{12} = E_{12} = \frac{\left(\gamma H + 4\pi^2\right)\left(\gamma H + \delta^2\right) Fe_2 r_0}{4\pi^2 \delta^2 \left(\gamma H + H + 4\pi^2\right)\left(\gamma H + H + \delta^2\right)} A_1^2.$$

Coefficient of ε^3

$$LM^{(3)} = [R_{31},\ R_{32},\ R_{33},\ R_{34},\ R_{35}]^{\mathrm{T}}, \tag{71}$$

where

$$R_{31} = \frac{1}{Pr} \frac{A_1}{\mathrm{d}\tau^*}, \quad R_{32} = \frac{\mathrm{d}B_{11}}{\mathrm{d}\tau^*} + A_1 D_{12} - Fe_2 r_2 A_1,$$
$$R_{33} = \frac{\mathrm{d}D_{11}}{\mathrm{d}\tau^*} - A_1 B_{12}, \quad R_{34} = \frac{\Gamma}{\delta^2 + \gamma H} \frac{\mathrm{d}C_{11}}{\mathrm{d}\tau^*}, \quad R_{35} = \frac{\Gamma}{4\pi^2 + \gamma H} \frac{\mathrm{d}E_{11}}{\mathrm{d}\tau^*}.$$

The Fredholm solvability condition applied to the third-order system gives us the Ginzburg–Landau equation:

$$\frac{\mathrm{d}A_1(\tau^*)}{\mathrm{d}\tau^*} = \frac{Pr^*}{1 + Pr^*} \left(P_1 A_1(\tau^*) - P_2 A_1(\tau^*)^3\right), \tag{72}$$

where

$$P_1 = \frac{\delta^2 \left(\delta^2 + \gamma H\right)\left(\delta^2 + H + \gamma H\right) r_2}{P_3}, \quad P_2 = \left(\frac{\left(\gamma H + 4\pi^2\right)(\delta^2 + \gamma H)^2}{4\pi^2 P_3 \left(\gamma H + H + 4\pi^2\right)}\right),$$
$$Pr^* = \frac{P_3 Fe_2 r_0}{\delta^4 \left(\delta^2 + H + \gamma H\right)^2} Pr, \quad P_3 = \delta^4 + \gamma^2 H^2 + \gamma H \left(\Gamma H + 2\delta^2\right).$$

References

Banu, N., Rees, D.A.S.: Onset of Darcy - Bénard convection using a thermal non-equilibrium model. Int. J. Heat Mass Transf. **45**, 2221–2228 (2002)

Barletta, A., Celli, M., Lagziri, H.: Instability of a horizontal porous layer with local thermal non-equilibrium: effects of free surface and convective boundary conditions. Int. J. Heat Mass Transf. **89**, 75–89 (2015)

Barletta, A., Rees, D.A.S.: Local thermal non-equilibrium effects in the Bénard instability with isoflux boundary conditions. Int. J. Heat Mass Transf. **55**, 384–394 (2012)

Bhadauria, B.S., Agarwal, S.: Convective transport in a nanofluid saturated porous layer with thermal non equilibrium model. Transp. Porous Med. **88**, 107–131 (2011)

Celli, M., Barletta, A., Storesletten, L.: Local thermal non-equilibrium effects in the Bénard instability of a porous layer heated from below by a uniform flux. Int. J. Heat Mass Transf. **67**, 902–912 (2013)

Celli, M., Lagziri, H., Bezzazi, M.: Local thermal non-equilibrium effects in the Horton–Rogers–Lapwood problem with a free surface. Int. J. Therm. Sci. **116**, 254–264 (2017)

Chandrasekhar, S.: Hydrodynamic and Hydromagnetic Stability. Oxford University Press, New York (1961)
Dehghan, M., Valipour, M.S., Saedodin, S.: Perturbation analysis of the local thermal non-equilibrium condition in a fluid-saturated porous medium bounded by an iso-thermal channel. Transp. Porous Med. **102**, 139–152 (2014)
Kaviany, M.: Principles of Heat Transfer in Porous Media. Springer, New York (2012)
Lagziri, H., Barletta, A., Celli, M., Bezzazi, M.: The onset of Darcy–Bénard instability in a horizontal porous channel with a free surface using a thermal nonequilibrium model. In: MATEC Web of Conferences, vol. 83, p. 07003 (2016)
Lapwood, E.R.: Convection of a fluid in a porous medium. Proc. Camb. Philos. Soc. **44**, 508–521 (1948)
Lee, J., Shivakumara, I.S., Mamatha, A.L.: Effect of nonuniform temperature gradients on thermogravitational convection in a porous layer using a thermal nonequilibrium model. J. Porous Med. **14**, 659–669 (2011)
Malashetty, M.S., Shivakumara, I.S., Kulkarni, S.: The onset of Lapwood–Brinkman convection using a thermal non-equilibrium model. Int. J. Heat Mass Transf. **48**, 1155–1163 (2005a)
Malashetty, M.S., Shivakumara, I.S., Kulkarni, S.: The onset of convection in an anisotropic porous layer using a thermal non-equilibrium model. Transp. Porous Med. **60**, 199–215 (2005b)
Nield, D.A., Kuznetsov, A.V., Xiong, M.: Effect of local thermal non-equilibrium on thermally developing forced convection in a porous medium. Int. J. Heat Mass Transf. **45**, 4949–4955 (2002)
Nield, D.A., Bejan, A.: Convection in Porous Media. Springer, New York (2006)
Nield, D.A.: A note on local thermal non-equilibrium in porous media near boundaries and interfaces. Transp. Porous Med. **95**, 581–584 (2012)
Nield, D.A., Kuznetsov, A.V.: Local thermal non-equilibrium and heterogeneity effects on the onset of convection in a layered porous medium. Transp. Porous Med. **102**, 1–13 (2014)
Nield, D.A., Kuznetsov, A.V., Barletta, A., Celli, M.: The onset of convection in a sloping layered porous medium: effects of local thermal non-equilibrium and heterogeneity. Transp. Porous Med. **114**, 87–97 (2016)
Postelnicu, A., Rees, D.A.S.: The onset of Darcy–Brinkman convection in a porous layer using a thermal nonequlibrium model part I: stress free boundaries. Int. J. Energy Res. **27**, 961–973 (2003)
Postelnicu, A.: The onset of a Brinkman convection using a thermal nonequilibrium model. Part II. Int. J. Therm. Sci. **47**, 1587–1594 (2008)
Rees, D. A. S., Pop, I.: Local thermal non-equilibrium in porous medium convection. Transp. Porous Med. III. (ed D. B. Ingham, I. Pop) 147–173 (2005)
Rees, D.A.S., Bassom, A.P., Siddheshwar, P.G.: Local thermal non-equilibrium effects arising from the injection of a hot fluid into a porous medium. J. Fluid Mech. **594**, 379–398 (2008)
Rudraiah, N., Siddheshwar, P.G., Masuoka, T.: Nonlinear convection in porous media: a review. J. Porous Media **6**, 1–32 (2003)
Saravanan, S., Sivakumar, T.: Onset of thermovibrational filtration convection: departure from thermal equilibrium. Phys. Rev. E **84**, 026307-1-13 (2011)
Shivakumara, I.S., Lee, J., Mamatha, A.L., Ravisha, M.: Boundary and thermal non-equilibrium effects on convective instability in an anisotropic porous layer. J. Mech. Sci. Technol. **25**, 911–921 (2011a)
Shivakumara, I.S., Lee, J., Vajravelu, K., Mamatha, A.L.: Effects of thermal nonequilibrium and non-uniform temperature gradients on the onset of convection in a heterogeneous porous medium. Int. Commun. Heat Mass Transf. **38**, 906–910 (2011b)
Siddheshwar, P.G., Vanishree, R.K., Kanchana, C.: Study of Rayleigh–Bénard–Brinkman convection using LTNE model and coupled, real Ginzburg–Landau equations. WASET. Int. J. Mech. Aero. Ind. Mech. Manuf. Eng. **11**, 1132–1139 (2017)
Siddheshwar, P.G., Kanchana, C.: Unicellular unsteady Rayleigh–Bénard convection in Newtonian liquids and Newtonian nanoliquids occupying enclosures: new findings. Int. J. Mech. Sci. **131**, 1061–1072 (2017)
Straughan, B.: Global nonlinear stability in porous convection with a thermal non-equilibrium model. Proc. R. Soc. Lond. A **462**, 409–418 (2006)
Straughan, B.: Green–Naghdi fluid with non-thermal equilibrium effects. Proc. R. Soc. Lond. A **466**, 2021–2032 (2010)
Straughan, B.: Convection with Local Thermal Non-Equilibrium and Microfluidic Effects. Springer, New York (2015)
Straus, J.M.: Large amplitude convection in porous media. J. Fluid Mech. **64**, 51–63 (1974)
Sunil, S.P., Mahajan, A.: Onset of Darcy-Brinkman ferroconvection in a rotating porous layer using a thermal non-equilibrium model: a nonlinear stability analysis. Transp. Porous Media. **88**, 421–439 (2011)
Vafai, K.: Handbook of Porous Media. CRC Press, London (2015)